Proceedings of the VIII International Conference ION 2010, Kazimierz Dolny, Poland, June 14–17, 2010

The Features of Real Part of Admittance in the Nanocomposites $(Fe_{45}Co_{45}Zr_{10})_x(Al_2O_3)_{100-x}$ Manufactured by the Ion-Beam Sputtering Technique with Ar Ions

T.N. Kołtunowicz[a,*], P. Zhukowski[a], V.V. Fedotova[b], A.M. Saad[c], A.V. Larkin[d] and A.K. Fedotov[d]

[a]Lublin University of Technology, Nadbystrzycka 38a, 20-618 Lublin, Poland

[b]Scientific-Practical Material Research Centre NAS of Belarus, P. Brovki 19, 220072 Minsk, Belarus

[c]Al-Balqa Applied University, P.O. Box 2041, Amman 11953, Jordan

[d]Belarussian State University, Independence 4, 220030 Minsk, Belarus

The temperature and frequency dependences of the admittance real part $\sigma(T, f)$ in granular $(Fe_{45}Co_{45}Zr_{10})_x(Al_2O_3)_{100-x}$ nanocomposite films around the percolation threshold x_C were investigated. The behaviour of $\sigma(T, f)$ vs. the temperature and frequency over the ranges 77–300 K and 50 Hz–1 MHz, respectively, displays the predominance of an activation (hopping) conductance mechanism for the samples below the percolation threshold x_C and of a metallic one beyond the x_C determined as 54 ± 2 at.%. The mean hopping range d for the nanoparticles diameter D was estimated at different metallic phase content x.

PACS: 79.20.Rf, 73.22.−f, 84.37.+q, 72.20.Ee

1. Introduction

Granular composite materials consisting of an insulating matrix mixed with the FeCo-containing soft ferromagnetic nanoparticles with different content x are used in various electromagnetic applications. In such binary composites the critical concentration, so-called percolation threshold x_C [1], is reached when a continuous current-conducting cluster of metallic particles is formed through the sample. In this case, when x is lower than x_C, a composite will be at the dielectric side of the metal–insulator transition (MIT), whereas at the values of x higher than x_C a composite will be at the metallic side of MIT.

Also, it should be noted that the majority of the electric, magnetic, and other properties of such binary nanocomposites are mostly influenced by the external effects just at x values approaching the percolation threshold x_C [2–4]. This feature makes these nanocomposites very attractive to the producers of various sensors, detectors, etc. The aim of this paper is (i) to investigate the electron transport mechanisms around the percolation threshold in granular nanocomposites consisting of nanoparticles of $Fe_{45}Co_{45}Zr_{10}$ alloy embedded into the amorphous dielectric alumina matrix using alternating current (AC) conductance measurements at different temperatures, and (ii) to extract some microscopic parameters of the electrons from these measurements.

2. Experimental

The films of $(Co_{45}Fe_{45}Zr_{10})_x(Al_2O_3)_{100-x}$ with 3–6 μm thickness were prepared by ion-beam sputtering of a complex target in a chamber evacuated with pure argon under the pressure $P_{Ar} = 0.7$–0.8 mPa. All the technological procedures and experimental techniques are described in [2–4]. The used method makes it possible to obtain a variety of samples under identical conditions but with different metallic phase concentrations ranging 30 at.% $< x <$ 65 at.%.

The synthesized films represent the double-phase systems, where metallic alloy nanoparticles are embedded into the dielectric Al_2O_3 matrix.

Our AC conductivity measurements were carried out with the same samples as for the measurements of direct current (DC) conductance, phase composition and magnetic state described in [2–4]. The previous measurements showed that the x_C value was close to 45–47 at.% [2].

The temperature and frequency dependences of the admittance for the samples were measured by means of the

* corresponding author; e-mail: t.koltunowicz@pollub.pl

two-probe method in the temperature range 77–340 K at the frequency range 50 Hz–1 MHz. This procedure is described in more detail in [5].

3. Results and discussion

Figure 1 presents the examples of the frequency dependences for real part of the admittance $\sigma(f)$ at temperatures 80–288 K in $(Fe_{45}Co_{45}Zr_{10})_x(Al_2O_3)_{100-x}$ nanocomposites with $x = 31.2$ at.% and $x = 64.1$ at.%.

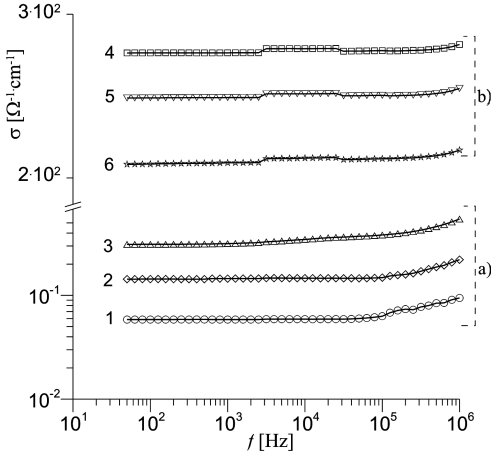

Fig. 1. Real part of the admittance σ for $(Co_{45}Fe_{45}Zr_{10})_x(Al_2O_3)_{100-x}$ nanocomposite as deposited vs. frequency with (a) $x = 31.2$ at.%, (b) $x = 64.1$ at.% determined at measuring temperatures T_p: 1 — 80 K, 2 — 138 K, 3 — 283 K, 4 — 80 K, 5 — 258 K, 6 — 283 K.

As can be seen in Fig. 1b, the observed $\sigma(T)$ dependences for the samples with $x > 54$ at.% are characteristic of metallic substances — they decrease with increasing temperature showing $\mathrm{d}\sigma/\mathrm{d}T < 0$. The value of the temperature coefficient for the resistivity α_ρ is typical of metallic substances and is equal to 4×10^{-4} K^{-1} for $x = 64.1$ at.%.

In the samples with $x < 54$ at.% the functions $\sigma(T)$ are opposite to the previous ones at all frequencies, increasing with a temperature growth to meet $\mathrm{d}\sigma/\mathrm{d}T > 0$ (see Fig. 1a).

The measurements conducted at the 77 K and at $f = 100$ Hz make it possible to build the $\sigma(x)$ dependence normalized to the value of $\sigma(100$ at.%) for a pure alloy sample, curve 1 in Fig. 2. It can be seen that this dependence can be presented as an intersection of two straight lines when a content of the metallic phase equals 54±2 at.%. This inflection point in the normalized $\sigma(x)/\sigma(x = 100$ at.%) curve (Fig. 2, curve 1) separates two different sets of samples with two different types of $\sigma(T)$ behaviour.

As follows from Fig. 3, at $x < 54$ at.% the studied samples are at the dielectric side of MIT (with $\mathrm{d}\sigma/\mathrm{d}T > 0$) with the activational $\sigma(T)$ dependences which are linear when plotted to the Arrhenius scale. At the same time,

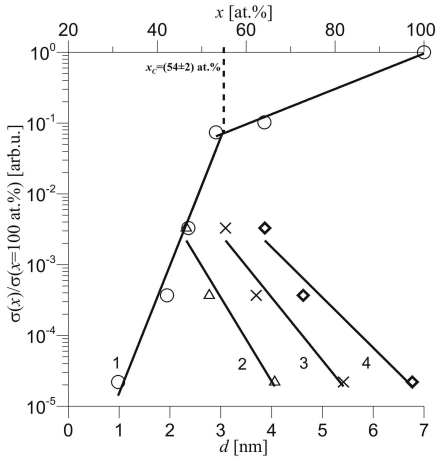

Fig. 2. Relative admittance $\sigma(x)/\sigma(x = 100$ at.%) vs. metallic phase content x (curve 1) and electron jump length d (curves 2, 3, 4). Measuring frequency — 100 Hz.

the samples with $x > 54$ at.% are at the metallic side of MIT, showing a nearly linear, power-law $\sigma(T)$ behaviour with $\mathrm{d}\sigma/\mathrm{d}T < 0$. This dielectric-to-metallic behaviour transition when crossing $x \approx 54 \pm 2$ at.% makes it possible to attribute the sense of the percolation threshold x_C to this value.

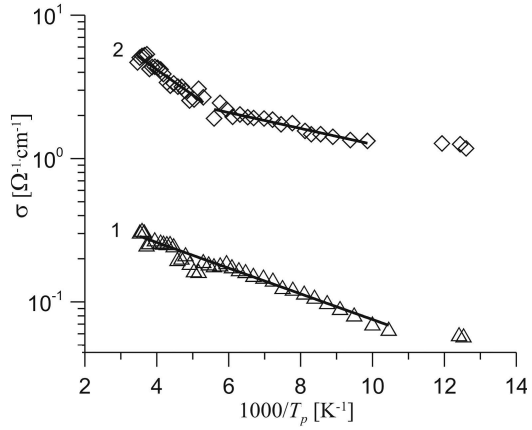

Fig. 3. Real part of the admittance vs. inverse temperature for the following metallic phase contents x: 1 — 31.2 at.%, 2 — 42.2 at.%. Measuring frequency — 100 Hz.

The amount of energy states in every metallic nanoparticle is equal to the number of atoms in the particle. Therefore, on the average, the energy "distance" ΔE between the neighbouring states, depending on the particle size D, is between 1 meV for $D = 6$ nm and 50 μeV for $D = 10$ nm. For a weak external electric field, the classical zone conductance in such particles must be close to zero. As noted by Imry in [6], for nanoparticles at relatively low temperatures the "dielectric"-type conductance with $\mathrm{d}\sigma/\mathrm{d}T > 0$ should be always observed, while in the

macroscopic systems one can observe $\mathrm{d}\sigma/\mathrm{d}T < 0$.

The analysis of the $\ln\sigma(1/T)$ dependences in Fig. 3 for the samples with $x = 31.2$ and 42.2 at.% confirms their "dielectric" behavior with $\mathrm{d}\sigma/\mathrm{d}T > 0$. The activation energies extracted from these linear dependences can be estimated around 10–30 meV. Taking this into account, we can assume that at the dielectric side of MIT ($x < x_\mathrm{C}$) the carrier transport is due to their hopping exchange between the neighboring nanoparticle states localized in the vicinity of the Fermi level. In this case conductance of nanocomposites can be described by the familiar relation (see [7]):

$$\sigma \sim \exp\left(-2\alpha_\mathrm{H} d - \frac{\Delta E}{kT}\right), \tag{1}$$

where d is the mean hopping range of electrons (mean distance between the centers of nanoparticles) and α_H — the rate of the electron wave function falling (reversal localization radius of electrons).

Since in Fig. 2 curve 1 is given for LNT, we can neglect the second component in (1) and reduce it to

$$\sigma \sim \exp\left(-2\alpha_\mathrm{H} d\right). \tag{2}$$

To determine the values of α_H from (2), we estimate the mean distance between the centers of nanoparticles d that is a function of x and hence of the mean nanoparticle dimension D. The transmission electron microscopy (TEM) and atomic force microscopy (AFM) study of such nanocomposites at the dielectric side of metal–dielectric transition (MDT) near the percolation threshold displayed the metallic alloy particles 6–10 nm in size [3]. At $x < x_\mathrm{C}$ the space between nanoparticles is filled with the matrix dielectric layers. If we suppose that nanoparticles are randomly distributed within the dielectric matrix and represent the spheres with diameters D, we can estimate the mean value of dielectric layer thickness d (see below).

At the determined volume content x of the metallic phase a number of atoms in a unit volume is about $N_M = 8.5 \times 10^{22}$ cm^{-3} [8]. In this case a number of atoms per nanoparticle is equal to $N_M x$. A number of Al_2O_3 molecules falling at $N_M x$ metallic atoms equals $N_M(1-x)$. In as much as the number of Al_2O_3 molecules in a unit volume is $N_D = 2.34 \times 10^{22}$ cm^{-3} [8], the volume of the dielectric phase is found from

$$\frac{N_M}{N_D}(1-x), \tag{3}$$

and the total volume of the nanocomposite sample is

$$V_\mathrm{N} = x + \frac{N_M}{N_D}(1-x). \tag{4}$$

Then the volume of the metallic phase in a unit volume of the nanocomposite (in cm^3) is given by

$$V_M = \frac{V_M}{V_M + V_D} = \frac{x}{x + \frac{N_M}{N_D}(1-x)}, \tag{5}$$

and a number of nanoparticles with the mean diameter D and the volume $V_n = \frac{\pi}{6}D^3$ in a unit volume of the nanocomposite (in cm^3) is determined by

$$n = \frac{V_M}{V_n} = \frac{6x}{\pi D^3\left[x + \frac{N_M}{N_D}(1-x)\right]}. \tag{6}$$

A mean distance between the centers of metallic nanoparticles amounts to

$$r \approx \frac{1}{\sqrt[3]{n}} = D\sqrt[3]{\frac{\pi\left[x + \frac{N_M}{N_D}(1-x)\right]}{6x}}. \tag{7}$$

The constant hopping range covered by the electron in the process of tunnelling to overcome the interparticle dielectric strata is equal to a thickness of the latter. Within the scope of the proposed model, a mean thickness of the dielectric strata between the neighbouring metallic nanoparticles, the centers of which are separated by the distance r (7), is given by

$$d = r - D = D\left[\sqrt[3]{\frac{\pi\left[x + \frac{N_M}{N_D}(1-x)\right]}{6x}} - 1\right]. \tag{8}$$

The estimated values of d obtained with formula (8) for the samples of $(Co_{45}Fe_{45}Zr_{10})_x(Al_2O_3)_{100-x}$ at x from 31.2 at.% to 64.1 at.% ($x < x_\mathrm{C}$) are represented in Fig. 2, curves 2, 3, 4, in the form of the normalized dependences $\sigma(d)/\sigma(x = 100$ at.%). As can be seen, this dependence is very well approximated by formula (2), that allows to extract the values of α_H which are estimated as 1.06 ± 0.25 nm^{-1} for D between 6 and 10 nm.

The conducted analysis confirms the presence of hopping conductance in the samples studied with $x < x_\mathrm{C}$. Moreover, a nonlinear increase in a real part of the admittance with frequency in Fig. 1 is apparent for hopping conductance only [9–12]. In the case of zone conductance we should have $\sigma(f) = \mathrm{const}$ at the dielectric side of MIT [7].

In both cases, the measured conductance is higher than expected value. This possibly means that at high concentrations of the metallic phase deposition of nanoparticles begins to occur in a correlated manner, forming a current conducting net of metallic nanoparticles. In this case a system of metallic nanoparticles becomes macroscopic, and the energy difference between the neighbouring states (levels) near the Fermi level decreases as 1 cm/10 nm $\approx 10^6$ compared to the isolated (individual) nanoparticles. This growth of the density of states at the Fermi level results in the transition from hopping conductance (by a tunnelling mechanism over the dielectric barrier) to the bulk band conductance as for the macroscopic metallic systems.

4. Conclusion

The frequency dependences of a real part of the admittance $\sigma(f)$ at different temperatures T in granular $(Fe_{45}Co_{45}Zr_{10})_x(Al_2O_3)_{100-x}$ nanocomposite films

around the percolation threshold x_C were investigated. The films were deposited using Ar ion-beam sputtering of the complex target containing $Fe_{45}Co_{45}Zr_{10}$ alloy and alumina stripes. Behaviour of the $\sigma(T, f)$ dependences for the samples studied in the ranges 77–300 K and 50 Hz–1 MHz displayed the predominance of an activation (hopping) conductance mechanism with $d\sigma/dT > 0$ for the samples below the percolation threshold determined as $x_C \approx 54 \pm 2$ at.%. Beyond x_C the samples revealed a metallic behaviour with power-like $\sigma(T)$ and $d\sigma/dT < 0$.

The features of $\sigma(T, f)$ dependences confirm hopping of electrons in the process of tunnelling over the dielectric barriers between the closest neighbouring metallic nanoparticles. The $\sigma(T, f)$ dependences made it possible to estimate the mean hopping ranges d and the rate of the wave function falling $\alpha_H \approx 1.06 \pm 0.25$ nm^{-1} of these electrons for different metallic phase contents 30 at.% $< x <$ 100 at.%.

Acknowledgments

The work was partially supported by the Fundation for Polish Science, VISBY Program of the Swedish Institute, Belarussian Fundamental Research Foundation by Contracts Φ06P-128 and Φ05 K-015 and the State Program of Belarus "Composition materials".

References

[1] D. Stauffer, A. Aharony, *Introduction to Percolation Theory*, Taylor and Francis, London 1992.

[2] A.M. Saad, A.K. Fedotov, J.A. Fedotova, I.A. Svito, B.V. Andrievsky, Yu.E. Kalinin, V.V. Fedotova, V. Malyutina-Bronskaya, A.A. Patryn, A.V. Mazanik, A.V. Sitnikov, *Phys. Status Solidi C* **3**, 1283 (2006).

[3] A.M. Saad, A.K. Fedotov, I.A. Svito, A.V. Mazanik, B.V. Andrievski, A.A. Patryn, Yu.E. Kalinin, A.V. Sitnikov, *Prog. Solid State Chem.* **34**, 139 (2006).

[4] A.M. Saad, A.K. Fedotov, I.A. Svito, J.A. Fedotova, B.V. Andrievsky, Yu.E. Kalinin, A.A. Patryn, V. Malyutina-Bronskaya, A.V. Mazanik, A. Sitnikov, *J. Alloys Comp.* **423**, 176 (2006).

[5] T. Kołtunowicz, *Elektronika — Konstrukcje Technologie Zastosowania* **10**, 37 (2007).

[6] Y. Imry, *Introduction to Mesoscopic Physics*, Oxford University Press, Oxford 2002.

[7] N.F. Mott, E.A. Davies, *Electronic Processes in Non-Crystalline Materials*, Oxford Press, Oxford 1979.

[8] A.F. Burenkow, F.F. Komarov, M.A. Kumakhov, M.M. Temkin, *Tables of Ion Implantation Spatial Distribution*, Gordon and Breach, New York 1986.

[9] P. Żukowski, T. Kołtunowicz, J. Partyka, Yu.A. Fedotova, A.V. Larkin, *Vacuum* **83**, S275 (2009).

[10] P. Żukowski, T. Kołtunowicz, J. Partyka, Yu.A. Fedotova, A.V. Larkin *Vacuum* **83**, S280 (2009).

[11] P. Żukowski, T. Kołtunowicz, J. Partyka, P. Węgierek, J.A. Fedotova, A.K. Fedotov, A.V. Larkin, *Przegląd Elektrotechniczny* **3**, 244 (2008).

[12] P. Żukowski, T. Kołtunowicz, J. Partyka, P. Węgierek, M. Kolasik, A.V. Larkin, J.A. Fedotova, A.K. Fedotov, F.F. Komarov, L.A. Vlasukova, *Przegląd Elektrotechniczny* **3**, 247 (2008).